

Advanced Electric Motor Technologies

**2D- and 3D-FEM-Analysis of
Axial Field Permanent Magnet Synchronous
Motors
– a Comparison (FEMAG-2D vs. FLUX-3D)**

Stefan PAINTNER, Maximilian PILZ, Dorin ILES

Ingenieurbüro Dr. Dorin ILES

FEMAG-Anwender-Treffen, Hannover 2014

- Short overview of the axial field PM synchronous machine technology highlighting the relevant aspects for modeling and analysis
 - diversity of configurations

- Comparison of modeling and analysis using a 2D- and a 3D-FEM approach

Main features

- D/L-ratio (short machines with large diameter, ideal for some applications)
- High inertia (flywheel)
- Modularity due to multi-stacking
- For larger diameter the number of poles can be easily implemented

Drawbacks

- strong axial magnetic stator-rotor attraction force
- mechanical design and manufacturing technology difficulties
 - bearing and imbalance
 - stator stack stamping and assembling
- power limitation of AxF-PMSM
 - for higher torque (i.e. larger outer diameter) the mechanical stress of the rotor-shaft interface becomes prohibitive
 - > multi-stack machines

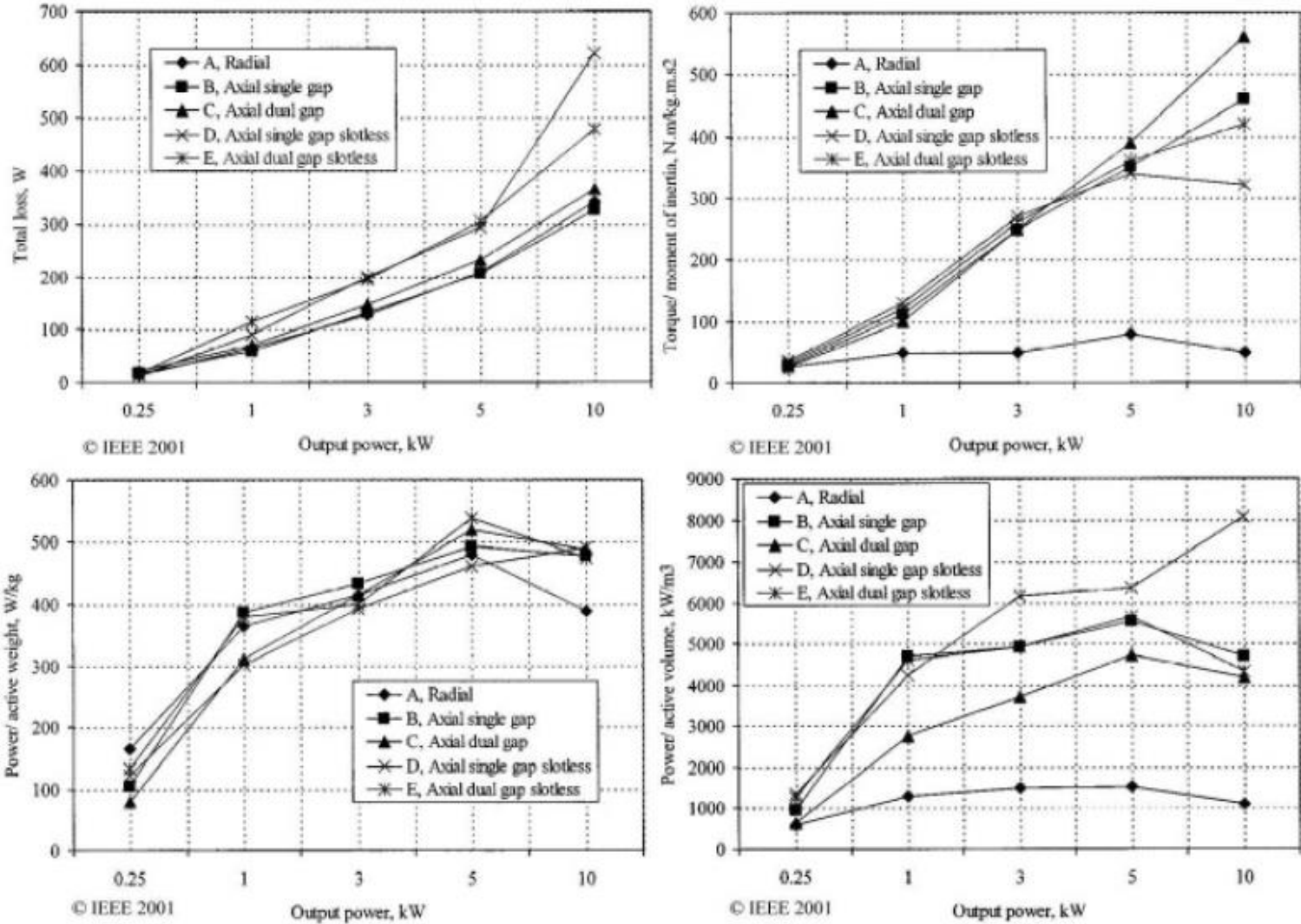
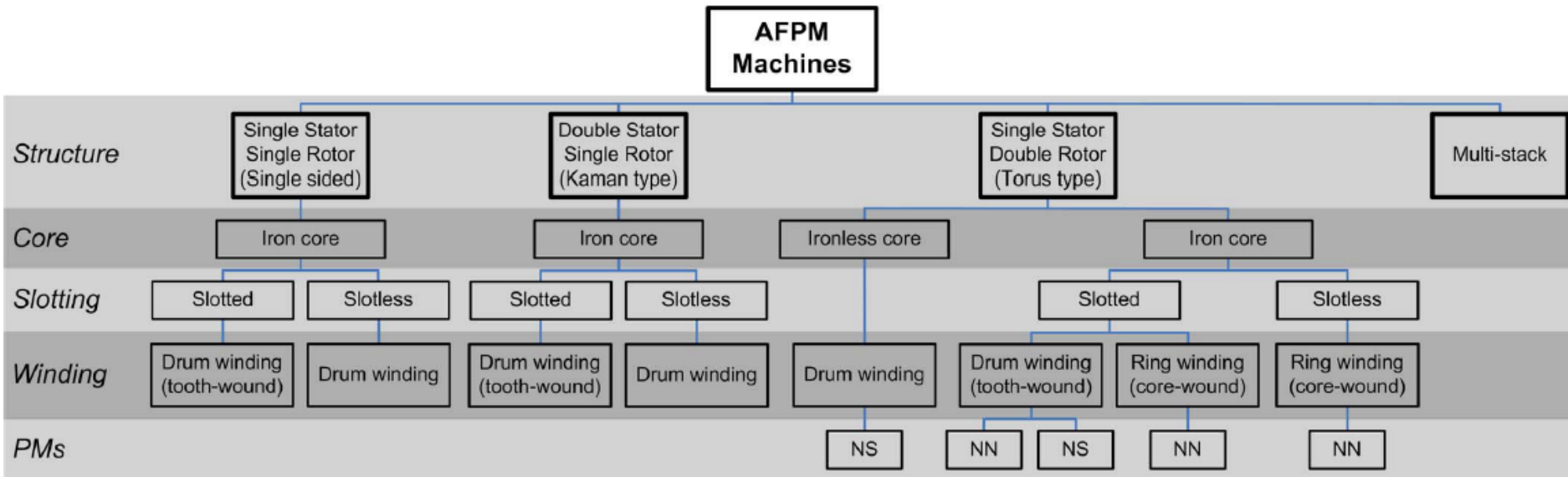
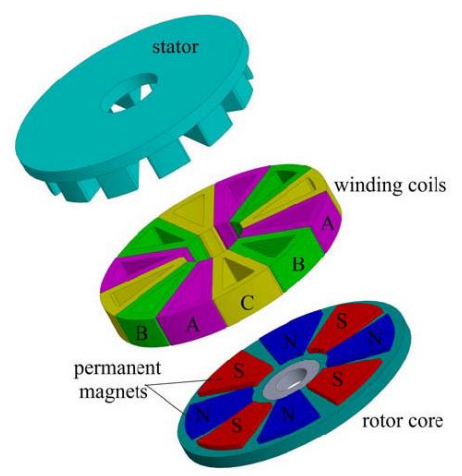


Figure 1.11. Performance comparison of RFPM and AFPM machines [214].

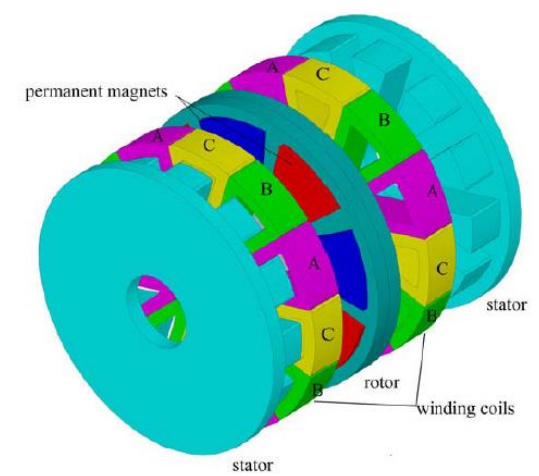
Sipati, IEEE

- Power generation
- Automotive
 - Traction for EV and HEV
 - Auxiliary drives (pumps, actuators, ...)
- Ship and submarine propulsion
- Electromagnetic aircraft launch systems
- Drill rigs, elevators
- Penny-motor
- Rotary actuators
- Vibration motors
- Hard disc drives
- Pumps in medical devices
- ...





3-D view of a four-pole-pair/12-slot SSSR AFPM machine



3-D view of a four-pole-pair/12-slot DSSR AFPM machine

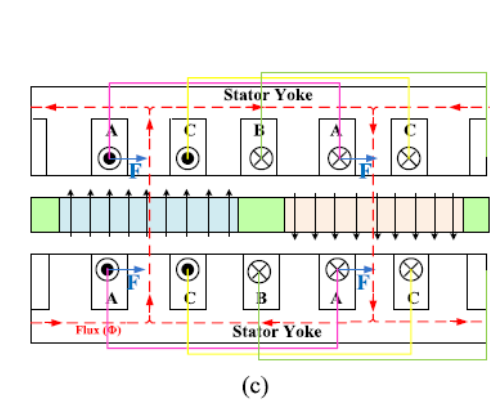
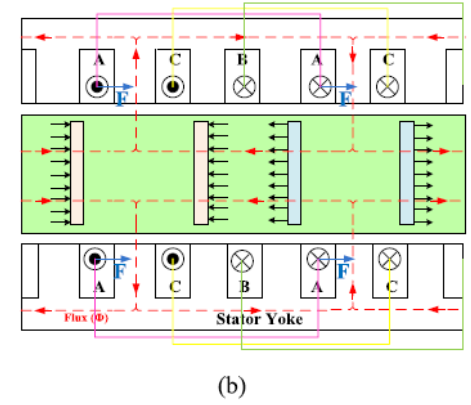
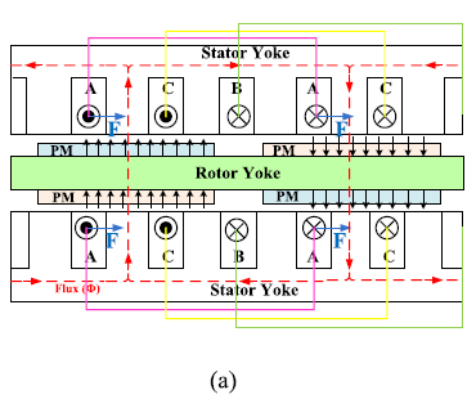
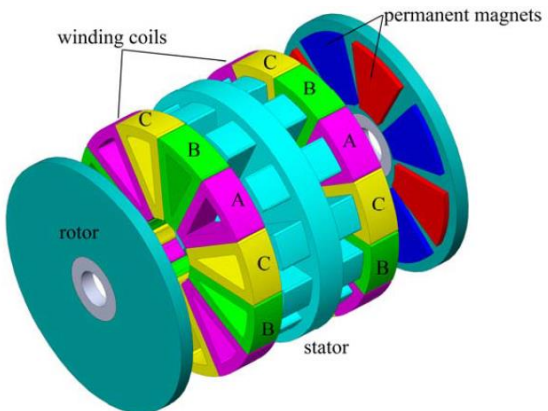


Fig. 4. Flux paths in 2-D plane for DSSR structure of the AFPM machine. (a) Surface-mounted PM structure. (b) Buried PM structure. (c) Interior PM structure without steel disc.



3-D view of a four-pole-pair/12-slot SSCR AFPM machine

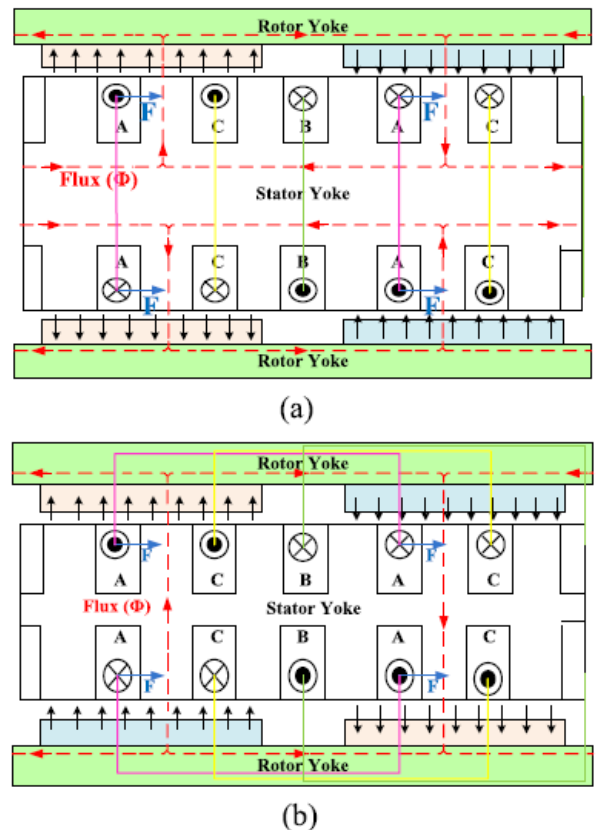
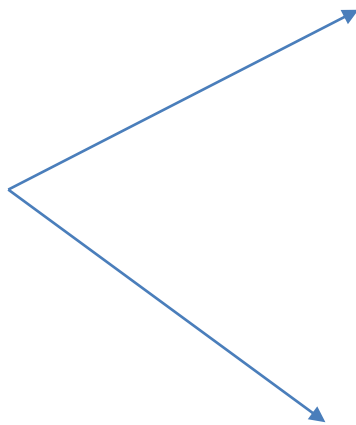


Fig. 6. Flux paths in 2-D plane for SSCR AFPM machine. (a) NN PM structure. (b) NS PM structure.

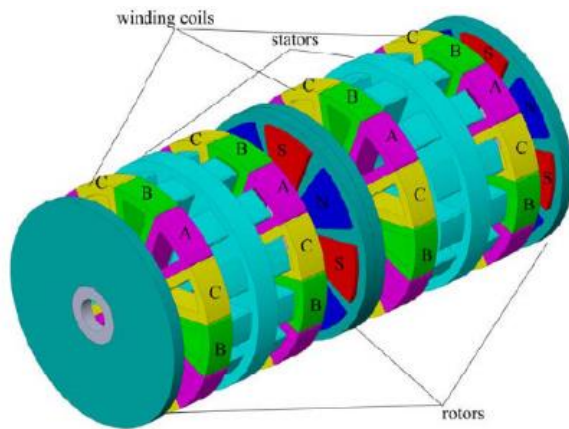
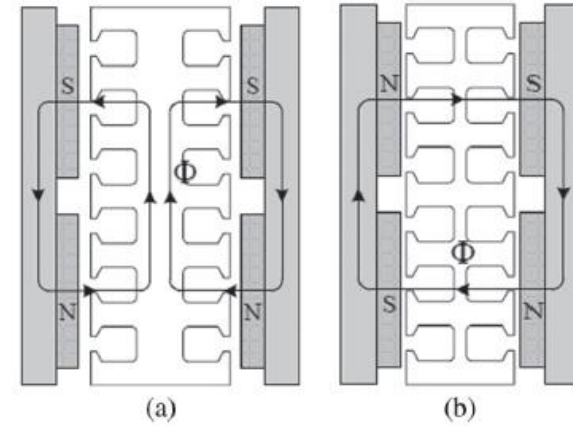
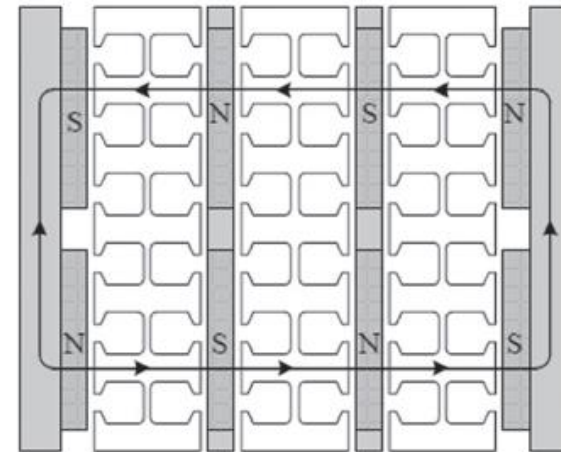


Fig. 8. 3-D view of a four-pole-pair/12-slot multistage AFPM machine ($N = 2$ stator; $N + 1 = 3$ rotors).



AFPM topologies: (a) Torus slotted NN and (b) Torus slotted NS



AFPM topologies: Torus slotted NS multi-stack [1].

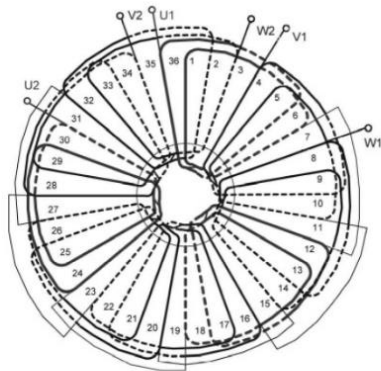


Figure 2.8. Single-layer winding of an AFPM machine with $m_1 = 3$, $2p = 6$, $s_1 = 36$, $y_1 = Q_1 = 6$ and $q_1 = 2$.

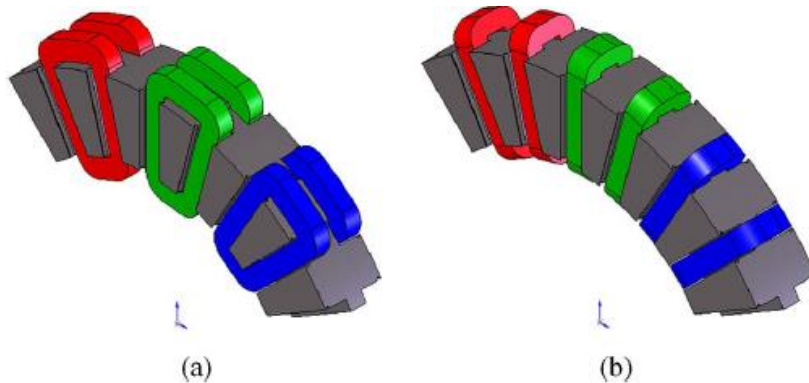


Fig. 2. AFPM winding types: (a) drum (tooth-wound) and (b) ring (core-wound) [46].

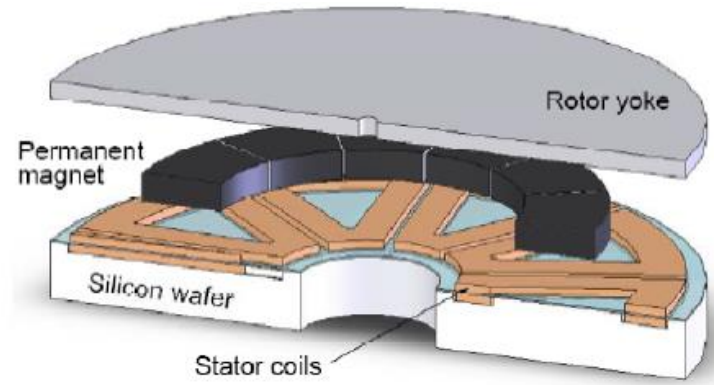


Fig. 1. Axial flux micro-motor: schematic (above) and stator picture

3D-Design



Figure 3.4. Powder salient pole stators for small single-sided AFPM motors. Technologies, LLC, West Lebanon, NH, U.S.A.

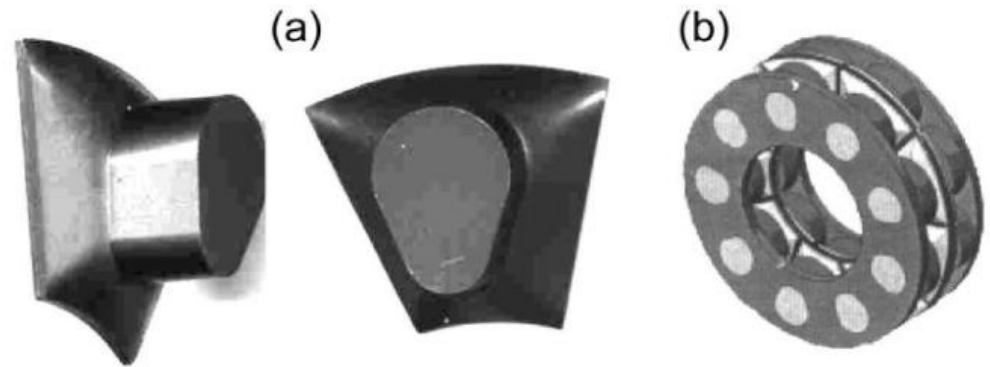
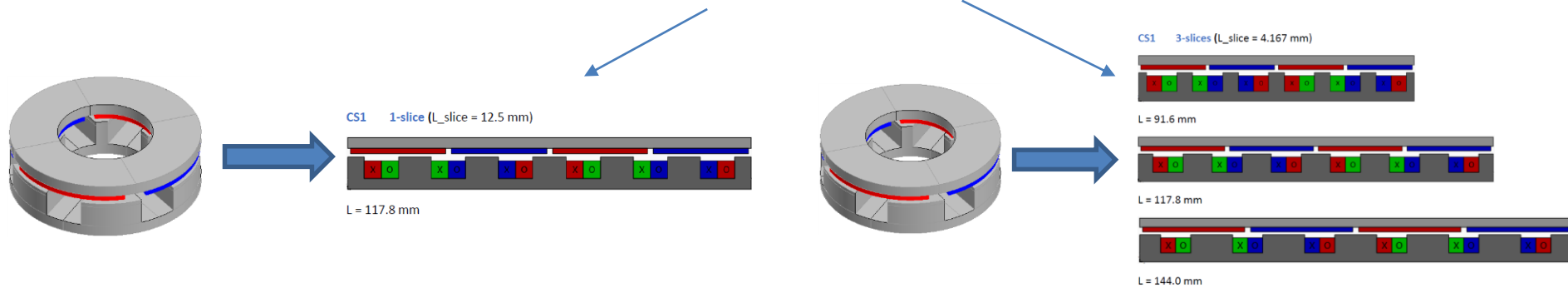


Figure 3.5. SMC powder salient pole for small single-sided AFPM motors: (a) single SMC pole; (b) double-sided AFPM motor. Courtesy of Höganäs, Höganäs, Sweden.

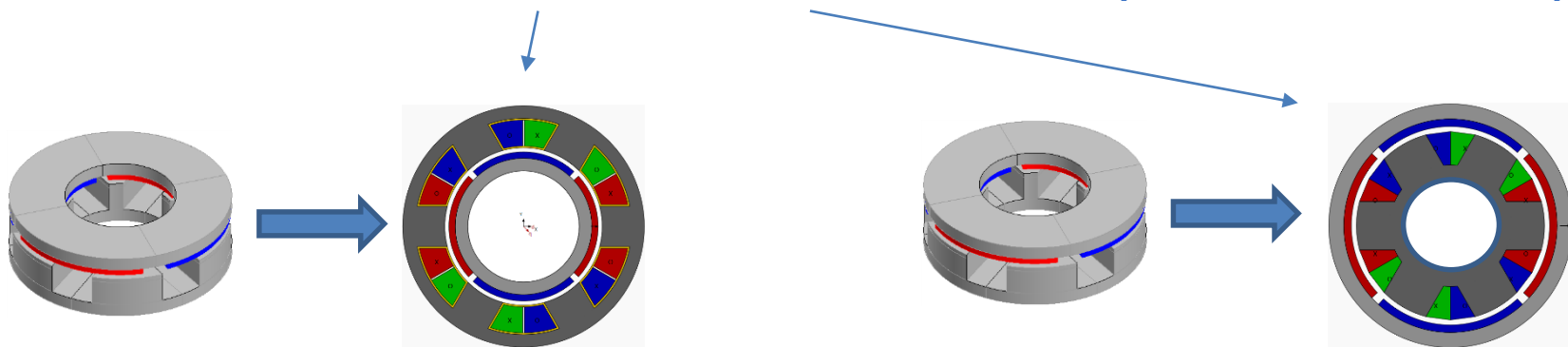
- Analytical (mainly for slotless configurations)
- NMEC (non-linear magnetic equivalent circuits, see literature)
- 2D-FE
- 3D-FE
- their multiple combinations (see literature)

- Use of homeomorphic (equivalent) topological transformation (without a change of the structure)

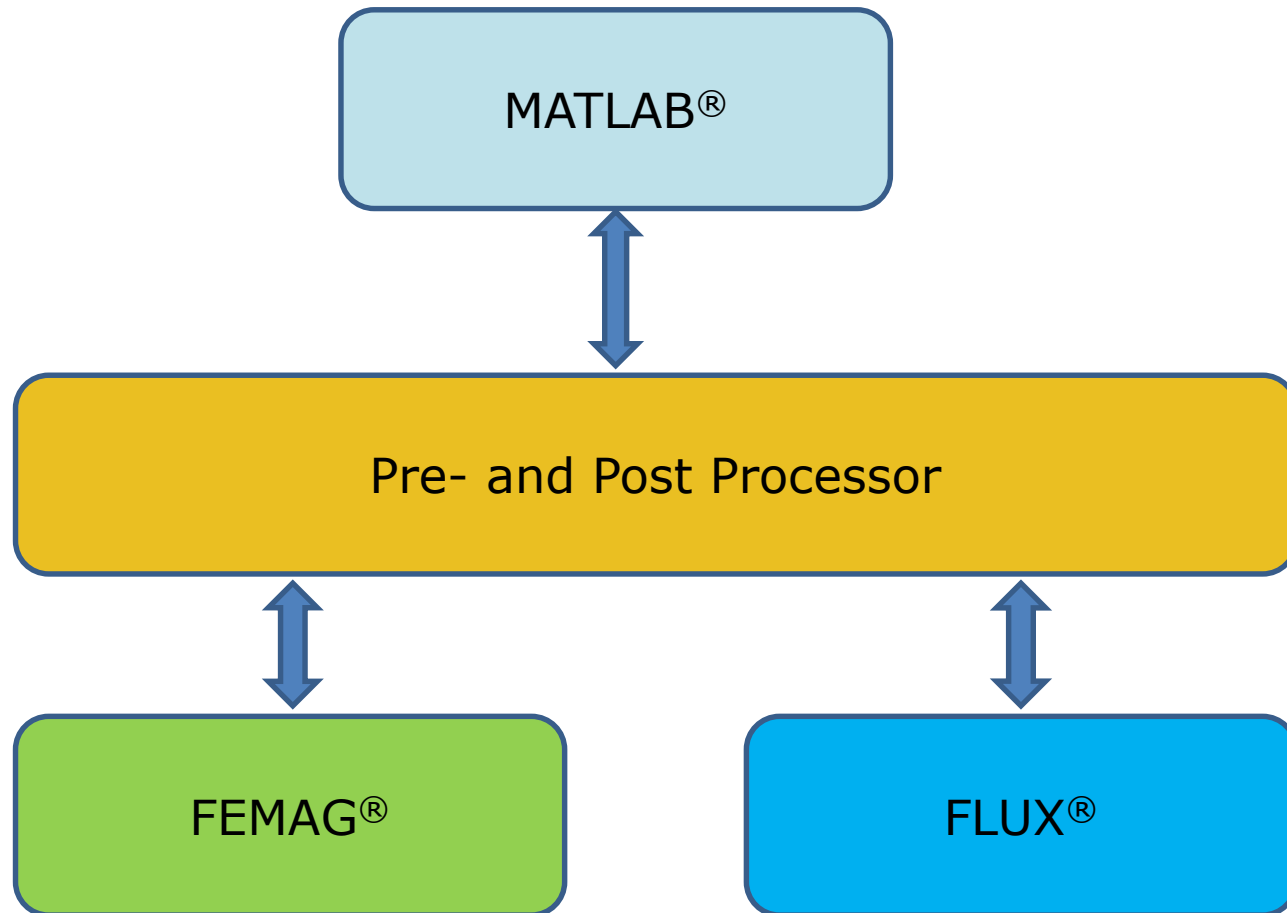
- AxF-PMMSM > Linear-PMMSM (one or more slices)



- AxF-PMMSM > Inner-/Outer-Rotor-PMMSM (one or more slices)

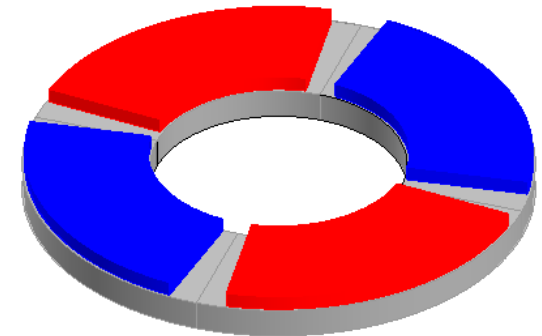
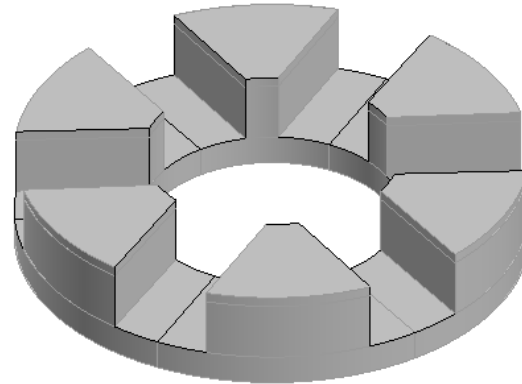
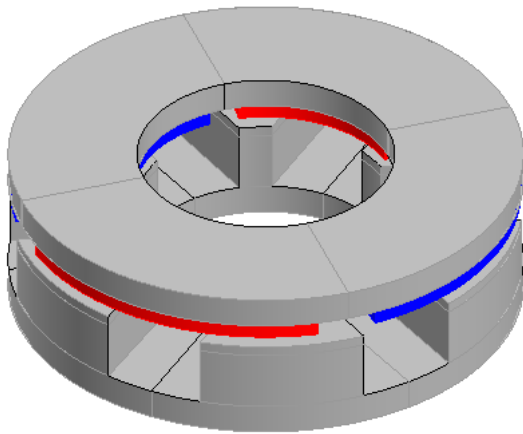


MATLAB-scripted Pre- and Postprocessor for FEMAG and FLUX



- AxF-PMSM without radial overhang in stator and/or rotor
 - Case study #1: AxF-PMSM / teeth without tooth-tip
 - M400-50A stator and sintered NdFeB-PM
 - Case study #2: AxF-PMSM / teeth with tooth-tip
 - M400-50A stator and sintered NdFeB-PM

- AxF-PMSM with radial overhang in stator and/or rotor
 - Case study #3: AxF-PMSM
 - SMC-stator and rotor flux concentration using hard ferrite PM



$n_s = 6$
 $n_p = 4$

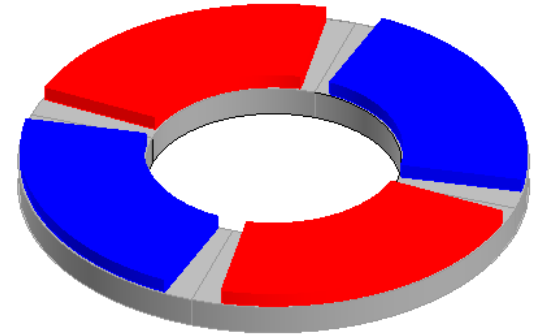
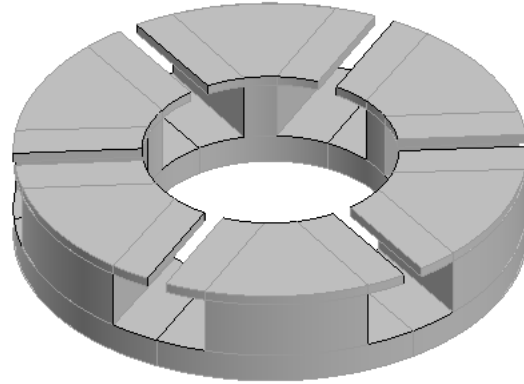
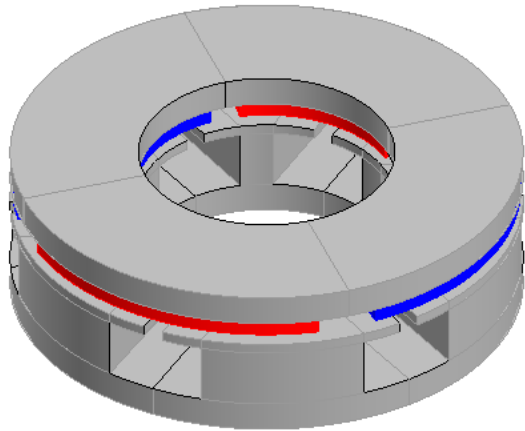
$D_{so} = 50 \text{ mm}$
 $D_{si} = 25 \text{ mm}$

$h_{yr} = 3 \text{ mm}$
 $h_{PM} = 1.5 \text{ mm}$
 $h_{ts} = 7 \text{ mm}$
 $h_{ys} = 3 \text{ mm}$
 $gap = 1 \text{ mm}$

S/R: M400-50A
 PM: Br20= 1.2 T

$n_{tc} = 10$
 $S_{fill} = 40 \%$

$n = 3000$
 $I_{ph_rms} = 7.0711$ (sinusoidal current controlled)



$n_s = 6$
 $n_p = 4$

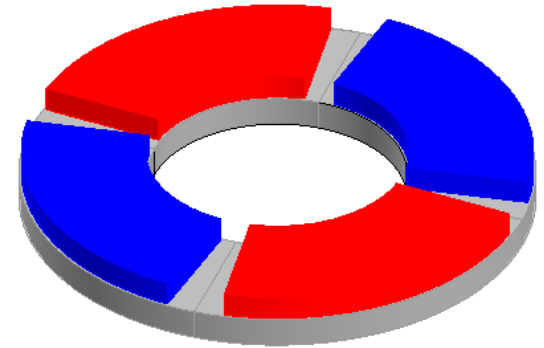
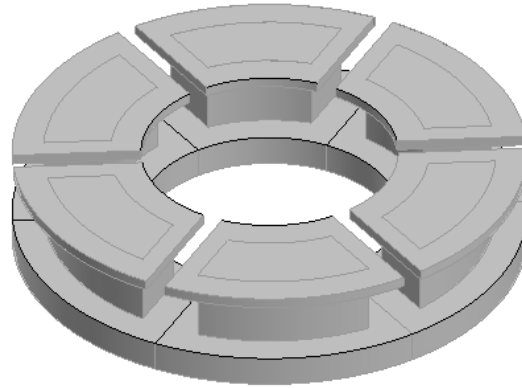
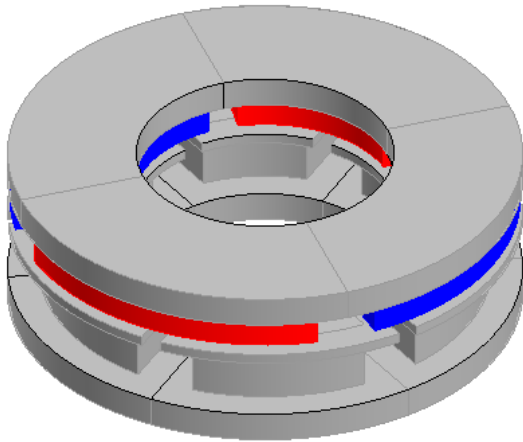
$D_{so} = 50 \text{ mm}$
 $D_{si} = 25 \text{ mm}$

$h_{yr} = 3 \text{ mm}$
 $h_{PM} = 1.5 \text{ mm}$
 $h_{ts} = 6 \text{ mm}$
 $h_{tt} = 1 \text{ mm}$
 $h_{ys} = 3 \text{ mm}$
 $gap = 1 \text{ mm}$

S/R: M400-50A
 PM: Br20= 1.2 T

$n_{tc} = 10$
 $S_{fill} = 40 \%$

$n = 3000$
 $I_{ph_rms} = 7.0711$ (sinusoidal current controlled)



$n_s = 6$
 $n_p = 4$

$D_{so} = 50 \text{ mm}$
 $D_{si} = 25 \text{ mm}$

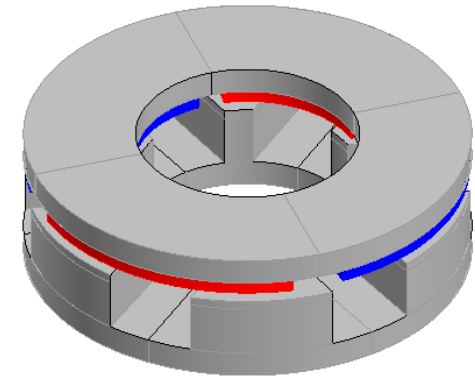
$h_{yr} = 3 \text{ mm}$
 $h_{PM} = 3.0 \text{ mm}$
 $h_{ts} = 6 \text{ mm}$
 $h_{tt} = 1 \text{ mm}$
 $h_{ys} = 3 \text{ mm}$
 $gap = 1 \text{ mm}$

S/R: SMC-Somaloy 500
 PM: Br20= 0.4 T

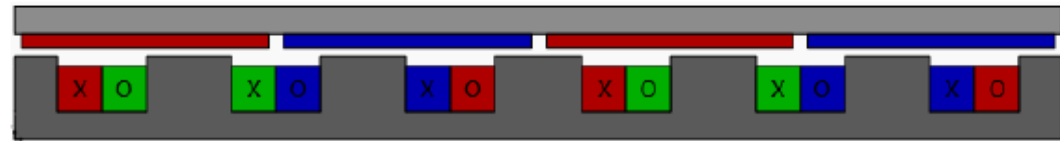
$n_{tc} = 10$
 $S_{fill} = 40 \%$

$n = 3000$
 $I_{ph_rms} = 7.0711$ (sinusoidal current controlled)

Modeling and analysis

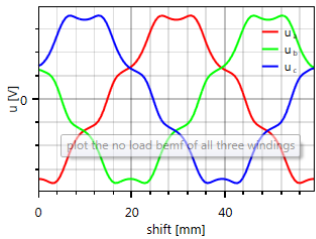


CS1 1-slice ($L_{\text{slice}} = 12.5 \text{ mm}$)

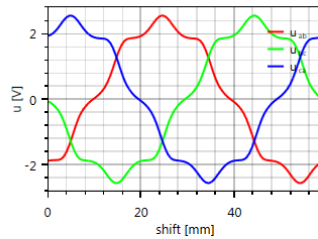


$L = 117.8 \text{ mm}$

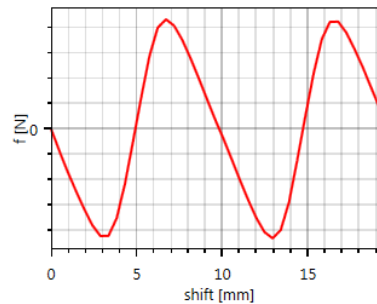
bemf ph



bemf ll

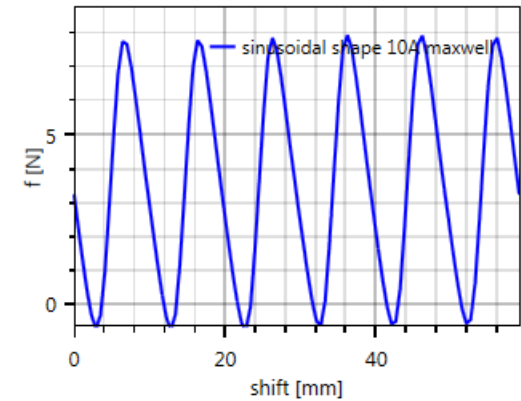


cogging

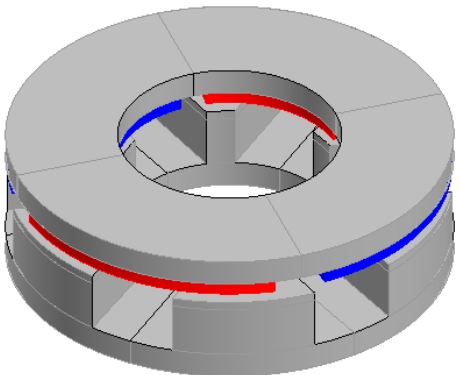


maxwell dpsi/dalpha

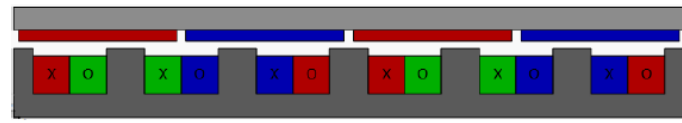
load



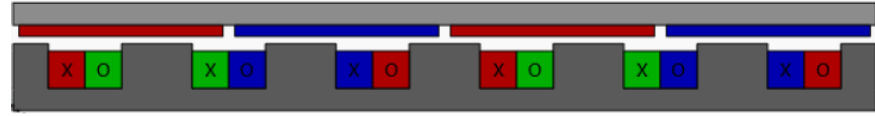
Modeling and analysis



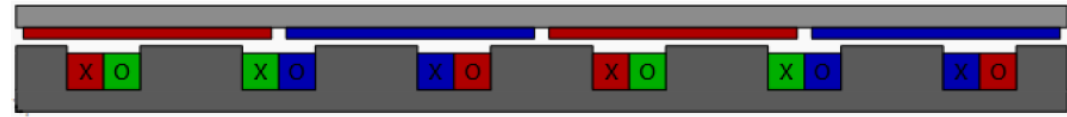
CS1 3-slices ($L_{\text{slice}} = 4.167 \text{ mm}$)



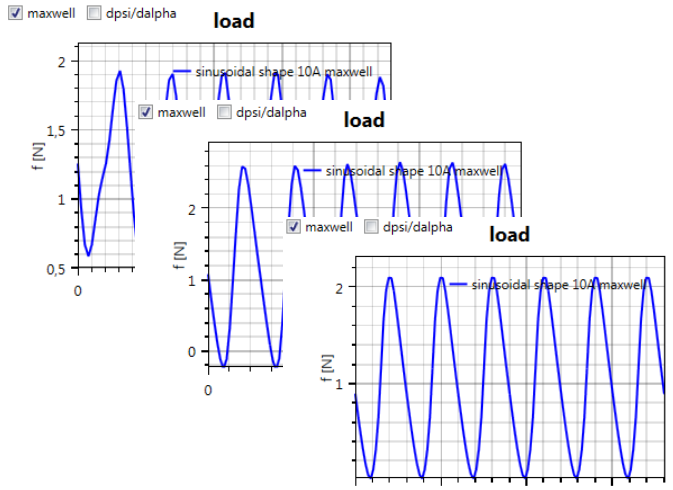
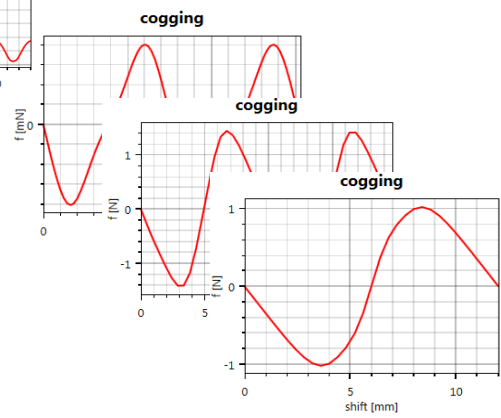
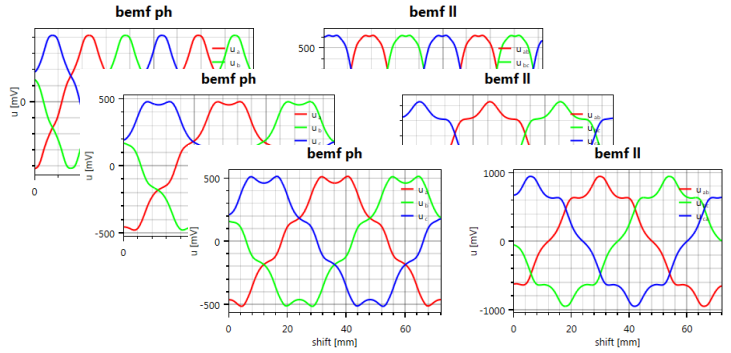
L = 91.6 mm



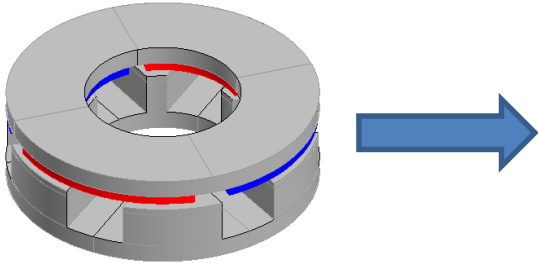
L = 117.8 mm



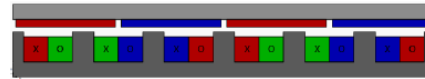
L = 144.0 mm



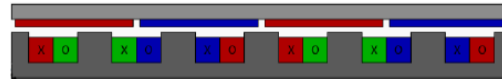
Modeling and analysis



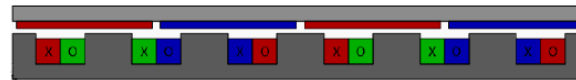
CS1 5-slices (L_{slice} = 2.5 mm)



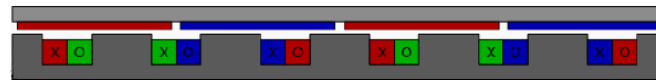
L = 86.5 mm



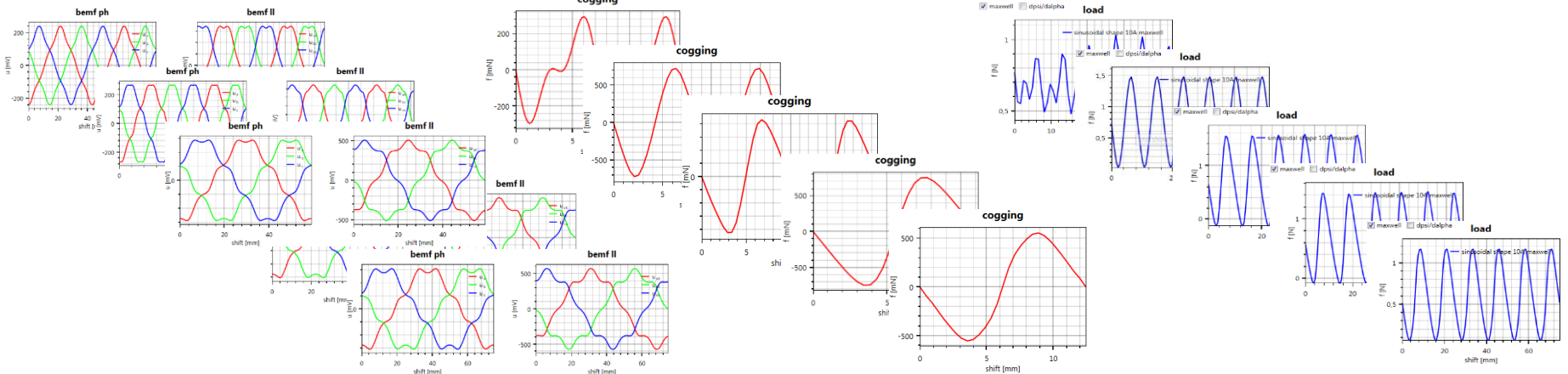
L = 102.1 mm



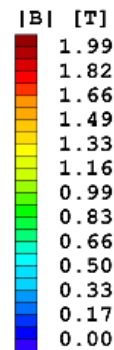
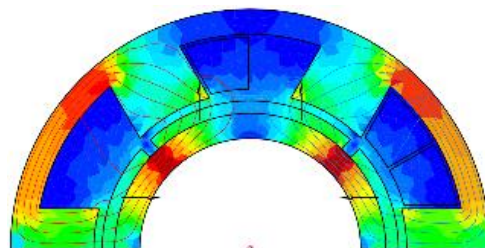
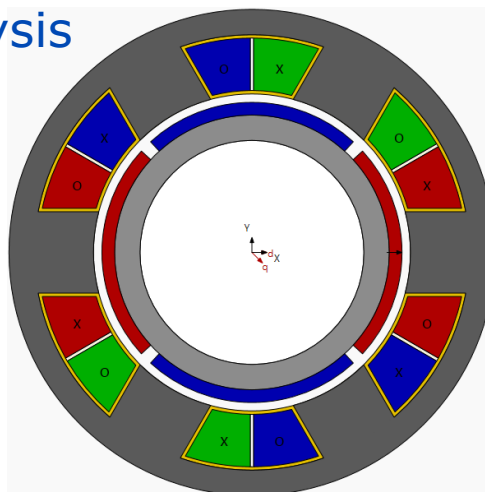
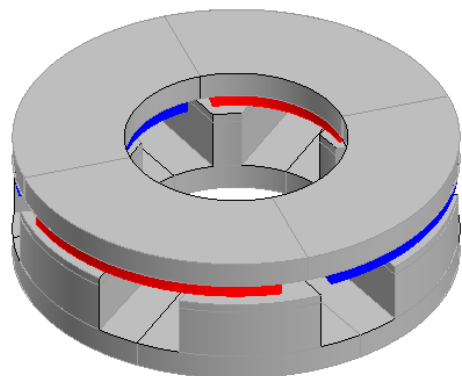
L = 117.8 mm



L = 133.5 mm



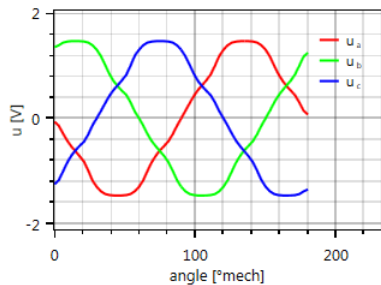
Modeling and analysis



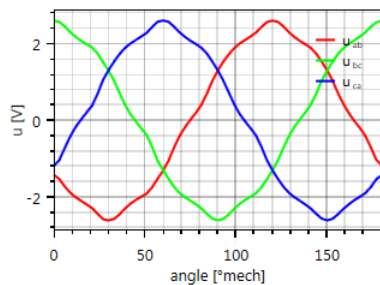
$D_{so} = 57.5 \text{ mm}$
 $D_{si} = 37.5 \text{ mm}$
 $L_{stk} = 12.5 \text{ mm}$

$h_{yr} = 3 \text{ mm}$
 $h_{PM} = 1.5 \text{ mm}$
 $h_{ts} = 7 \text{ mm}$
 $h_{ys} = 3 \text{ mm}$
 $gap = 1 \text{ mm}$

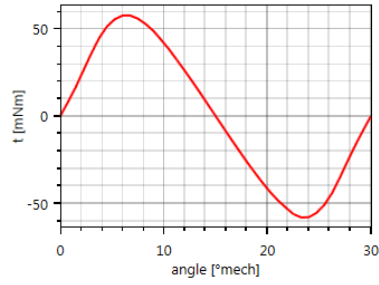
bemf ph



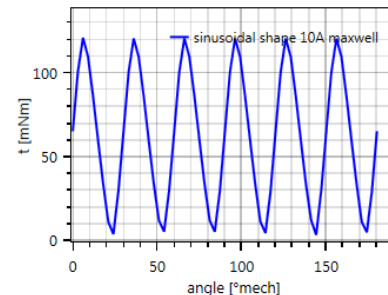
bemf ll



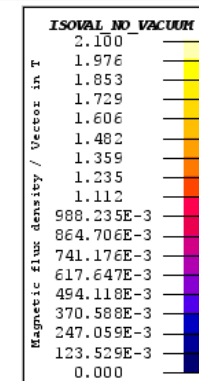
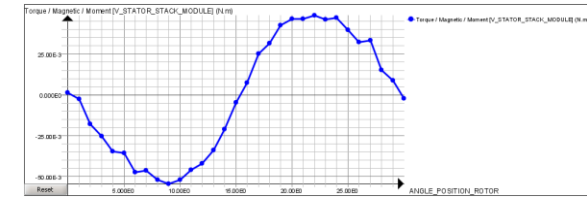
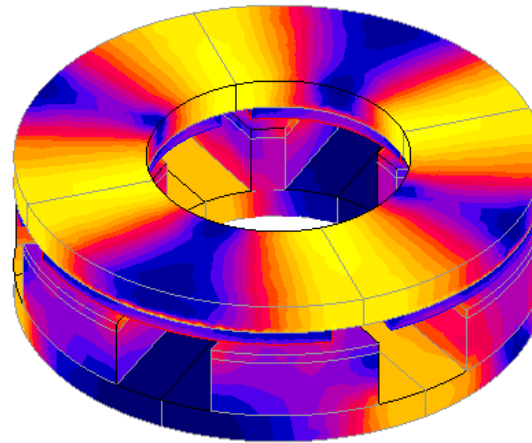
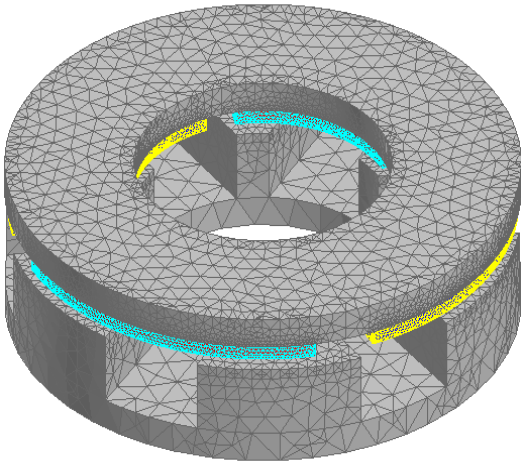
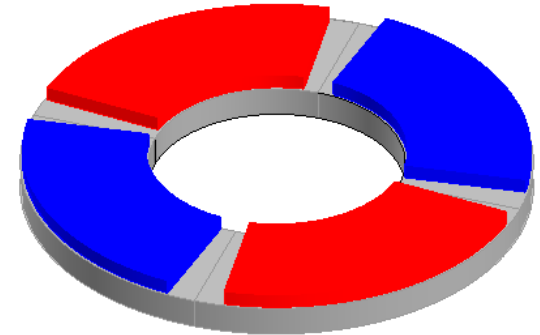
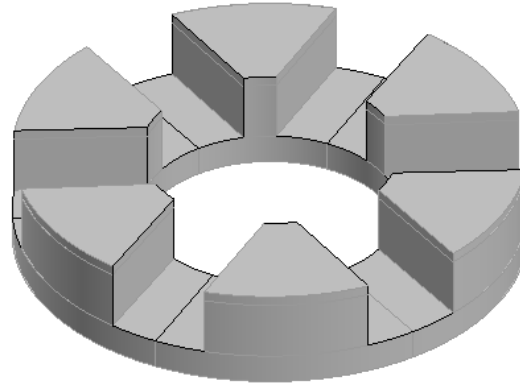
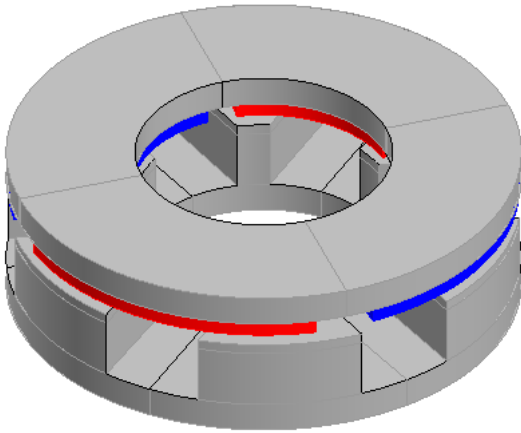
cogging



maxwell dps/dalpha **load**

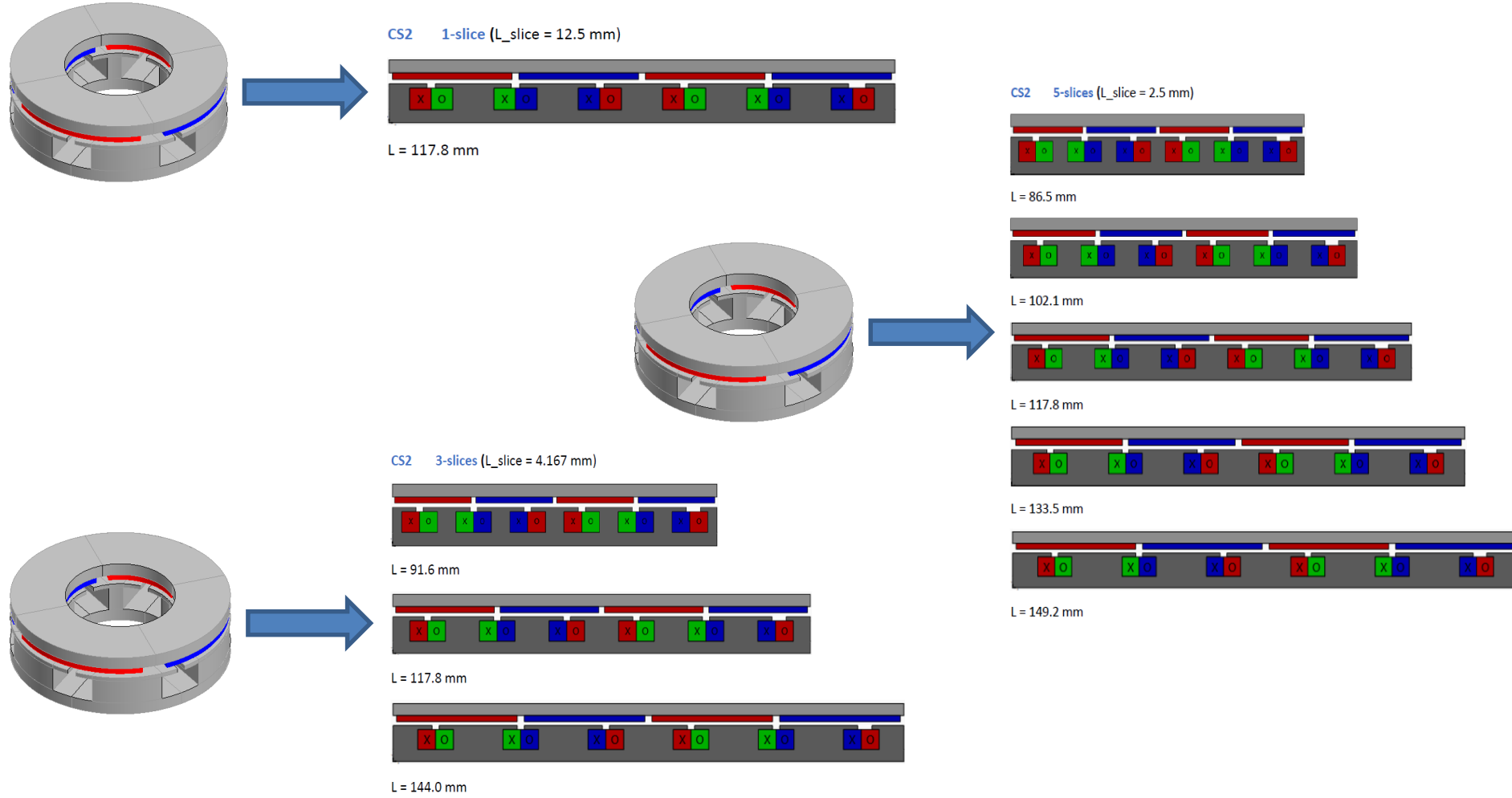


Modeling and analysis

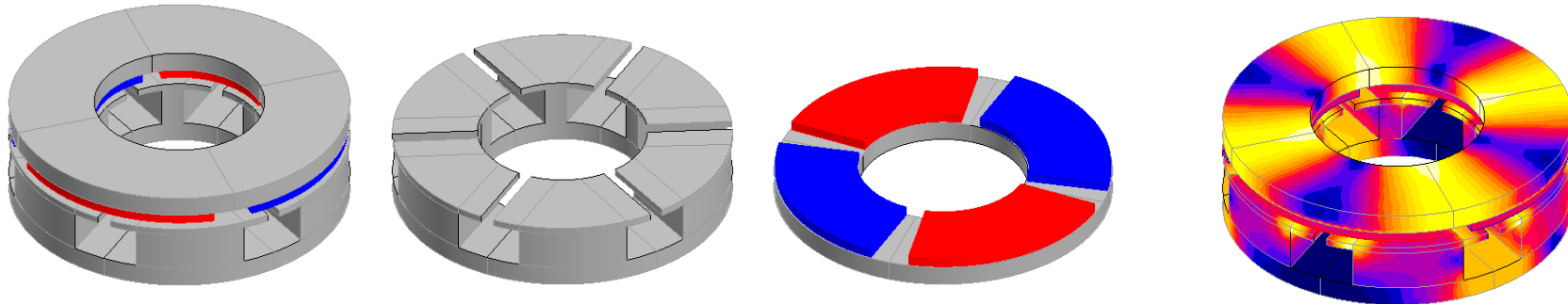
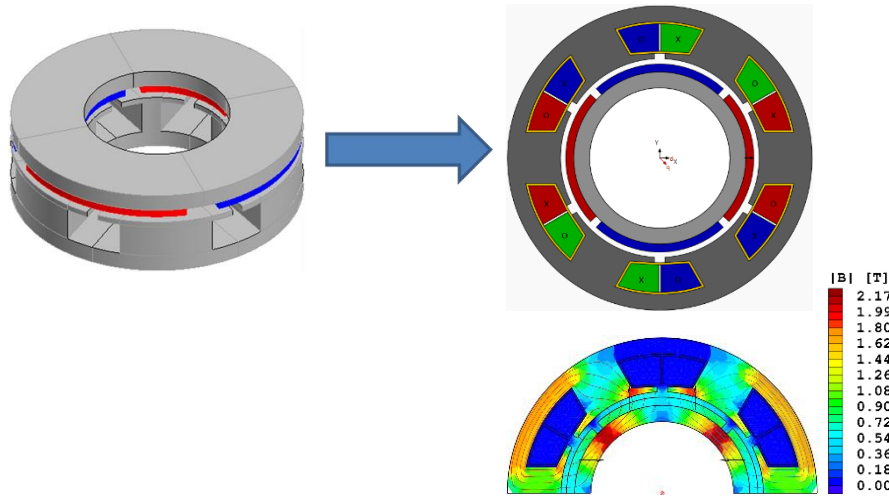


Mesh: 181059 volume elements
 Computation time: about 100 min.

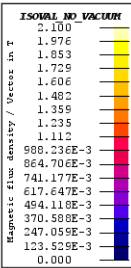
Modeling and analysis – similar approach



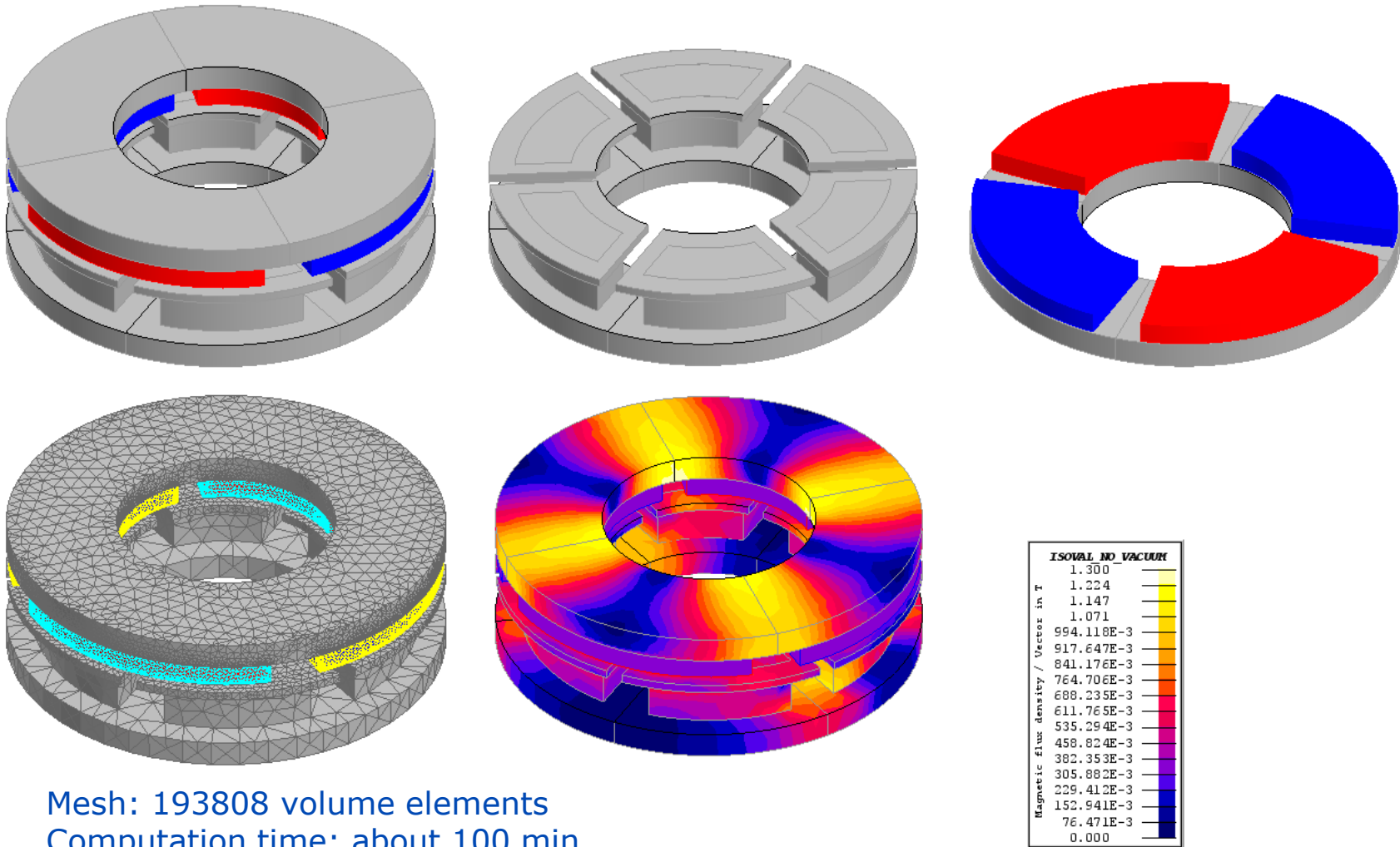
Modeling and analysis – similar approach



Mesh: 181059 volume elements (same FEM-Model used)
 Computation time: about 100 min.



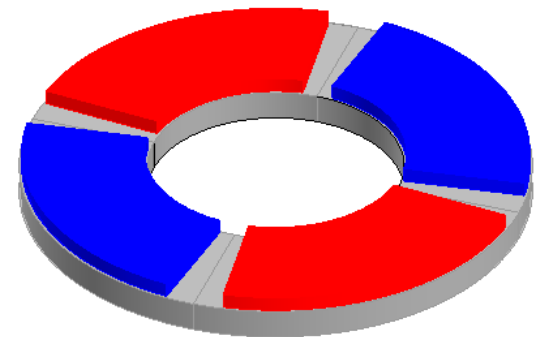
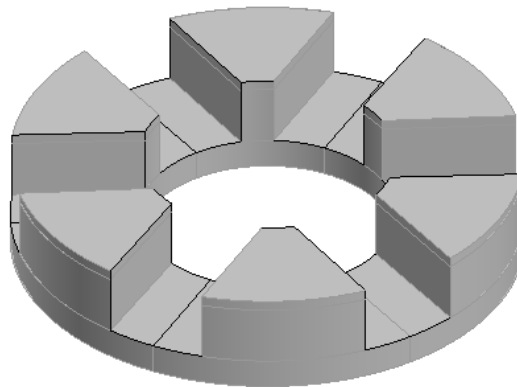
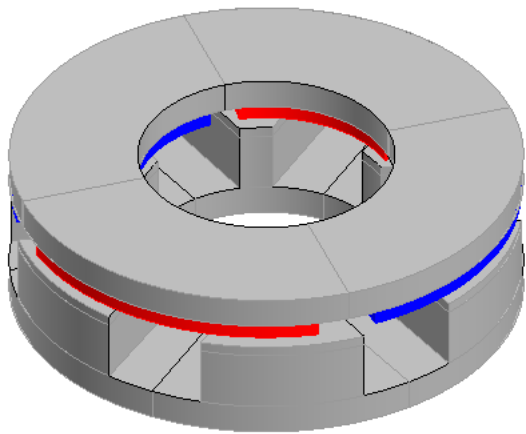
3D-FE-approach – mandatory



Mesh: 193808 volume elements
 Computation time: about 100 min.

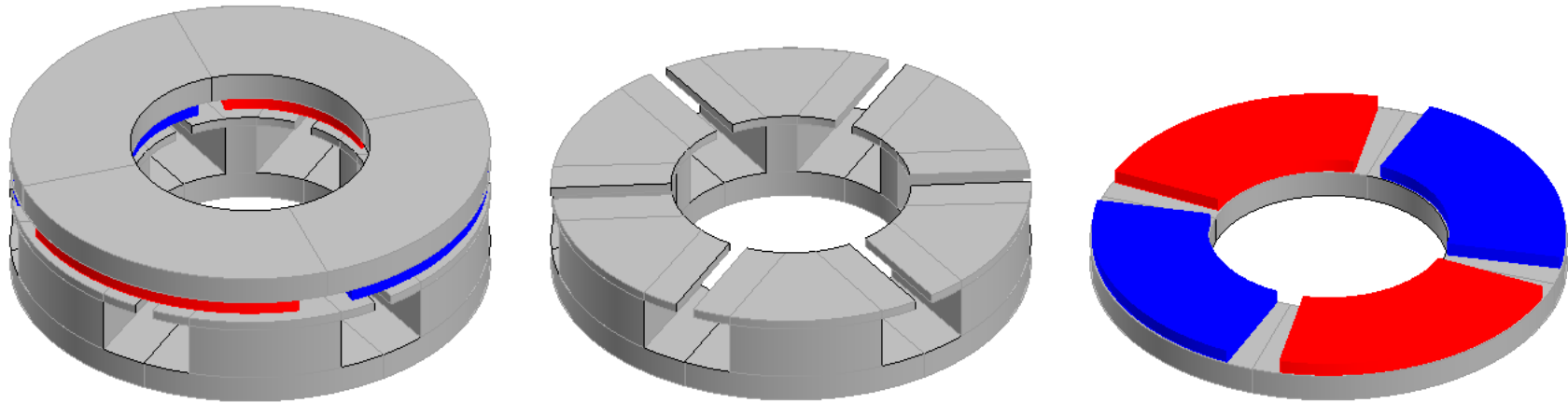
Approach	CS 1				
	2D-FE-linear			2D-FE-IR 1-slice	3D-FE
	1-slice	3-slices	5-slices		
Psi_PM* [%]	2.5	-1.6	-1.6	8.3	0.0
Tshaft* [%]	2.7	-1.7	-1.7	5.0	0.0
eta_motor* [%]	0.4	-0.3	-0.3	-1.6	0.0
Tcogg_pk-pk* [%]	58.4	10.9	5.6	13.0	0.0

* - relative deviation, 3D-FE = 100 %



Approach	CS 2				
	2D-FE-linear			2D-FE-IR 1-slice	3D-FE
	1-slice	3-slices	5-slices		
Psi_PM* [%]	-2.0	-4.1	-4.5	5.1	0.0
Tshaft* [%]	-2.3	-4.5	-5.0	5.2	0.0
eta_motor* [%]	-0.4	-0.8	-0.9	0.7	0.0
Tcogg_pk-pk* [%]	42.6	11.1	6.6	18.0	0.0

* - relative deviation, 3D-FE = 100 %



- AxF-PMSM without radial overhang in stator and/or rotor
 - 2D-FE linear machine approach
 - accuracy:
 - 3-slices: good
 - 5-slices: very good
 - 2D-FE-IR approach
 - Accuracy:
 - coarse fast estimation (no special tools requirement)
 - 3D-FE approach is necessary for a higher accuracy
- AxF-PMSM with radial overhang in stator and/or rotor
 - 3D-FE approach is mandatory

1. Gieras, Jacek F., Wang, Rong-Jie, Kamper, Maarten J., Axial Flux Permanent Magnet Brushless Machines, Springer 2008
2. Capponi, De Donato, Caricchi, Recent advances in axial-flux permanent-magnet machine technology, IEEE
3. Alipour, Moallem, Analytical magnetic field analysis of axial flux permanent-magnet machines using Schwarz-Christoffel transformation, IEEE
4. Koechli, Perriard, Analytical model for slotless permanent magnet axial flux motors, IEEE
5. Abbaszadeh, Maroufian, Axial flux permanent magnet motor modeling using magnetic equivalent circuit, IEEE
6. Maloberti et al., 3D-2D dynamic magnetic modeling of an axial flux permanent magnet motor with soft magnetic composites for hybrid electric vehicles, IEEE
7. Kahourzade et al., A comprehensive review of axial-flux permanent-magnet machines, IEEE
8. Choi et al., Electromagnetic Analysis of double-sided axial flux permanent magnet motor with ring-wound type slotless stator based on analytical modeling, IEEE
9. Garcia, Escudero, 2D analytical calculation of the open circuit electromagnetic field distribution in an axial flux slotted permanent magnet machine using fourier analysis, IEEE
10. Gair, Canova, A new 2D FEM analysis of a disc machine with offset rotor, IEEE
11. Zhilichev, Three-dimensional analytic model of permanent magnet axial flux machine, IEEE
12. Bumby et al., Electromagnetic design of axial-flux permanent magnet machines, IEEE
13. Parvianen, Niemelä, Pyrhönen, Modeling of axial flux permanent-magnet machines, IEEE
14. Fei, Luk, Jinupun, A new axila flux permanent magnet segmented-armature-torus machine for an in-wheel direct drive application, IEEE

15. Chan, Lai, Xie, Field computation of axial flux permanent-magnet synchronous generator, IEEE
16. Boccaletti, Di Felice, Petrucci, Santini, A mathematical model of axial flux disc machines, IEEE
17. Fei, Luk, Torque ripple reduction of axial flux permanent magnet synchronous machine with segmented and laminated stator, IEEE
18. Kowal, Sergeant, Dupre, Van den Bossche, Comparison of nonoriented and grain-oriented material in an axial flux permanent-magnet machine, IEEE
19. Xia, Jin, Shen, Zhang, Design and analysis of an air-cored axial flux permanent magnet generator for small wind power application, IEEE
20. Tiegna, Bellara, Amara, Barakat, Analytical modeling of the open-circuit magnetic field in axial flux permanent-magnet machines with semi-closed slots, IEEE
21. Egea et al., Axial-flu-machine modeling with combination of FEM-2-D and analytical tools, IEEE
22. Jang et al., Characteristic analysis on the influence of misaligned rotor position of double-sided axial flux permanent magnet machine and experimental verification, IEEE
23. Sipati, Krishnan, Performance comparison of radial and axial field permanent magnet brushless machines, IEEE